

# A DFT Study the Electronic, Optical and Thermal Properties of XTe (X= Pb, Cd, Nb) for optoelectronic device Applications

Mohammed Zorah<sup>1\*</sup>

<sup>1</sup> Department of C. T. E, Imam Alkadhim University College, Baghdad, Iraq.

Corresponding author's: [moh.n.z1971@gmail.com](mailto:moh.n.z1971@gmail.com)

## ABSTRACT:

A First-principles based study to investigate the different properties of telluride (Te) based materials XTe (X= Pb, Cd, Nb) such as structural, electronic, optical, and thermal properties. The bandgap of XTe (X= Pb, Cd, Nb) was originate significantly decrement from 1.50 eV to 0.00 eV. Under the First-principles exploration Pb, Cd, and Nb are appropriate periodic elements for bandgap decrement in XTe materials. The bandgap nature was obtaining direct furthermore bandgap show that materials are proficient semiconductors. Niobium (Nb) is more advantageous than Pb and Cd. By substituting of X= Pb, Cd, Nb at the corner sites in XTe (X= Pb, Cd, Nb) additional gamma sites were participated in the electronic energy band gap ( $E_g$ ). It is also examined that optical peaks shifted toward larger energy due to decrement in the band gap. Thermal impact on macroscopic properties of XTe (X= Pb, Cd, Nb) compounds are predicted using the quasi-harmonic Debye model. The variations of the enthalpy (U-U), entropy (S-S), heat capacity, Debye temperature, and free energy with temperature function are obtained successfully. Moreover, small band-gap semiconducting Telluride (Te) based materials reveal low thermal conductivities at a prominent temperature which is curious for simple cubic structured materials. These compounds for electrical, optical, and thermal properties have made them practical novel materials for optoelectronic device applications.

**Keywords:** Telluride (Te) based compounds, Electronic, Structural, Optical, optoelectronic, CASTEP software

## 1. Introduction:

Telluride (Te) based compounds have received abundant consideration in recent decades owing to their simple cubic symmetries and variety of physical properties, which allow them to be used in a range of applications. Telluride (Te) based compounds show a extensive variety of applications including semiconducting and half metallic behavior furthermore ferroelectric, ferromagnetic and potentially multi-ferroic phases. Outstanding physicochemical characteristics make them ideal for a prominent application comprehended ferroelectricity, high charge ordering, giant magneto-resistance, magneto-transport,

piezoelectricity and thermoelectric properties [1-2]. The remarkable cubic structure present efficient functionalities in optoelectronics field as well as enormous projection for novel thermo-electric devices [3-5]. These compounds exhibit efficient and remarkable theoretical considerations aimed to learn the physical fact behind the electronic optical and thermal behavior [6].

They are predicting some incoming facts of XTe (X= Pb, Cd, Nb) accessible as a novel object for energy-saving, sensors, solar cells, fuel cells and other optoelectronic devices. Outstanding physical-thermal characteristics related XTe (X= Pb, Cd, Nb) compounds make them ideal for an extensive range of advanced applications as well as high-temperature electrical conductivity, charge transportation, magneto-transport piezoelectricity, and ferroelectricity properties [7]. The Quantum dots shape of (CdTe) materials is an efficient semiconductor due to few nano-scale in size and controlled shape. The CdTe semiconductor materials belong to group II-IV in periodic trend with excellent characteristics to current fluorophores. The proficient optical characteristics of CdTe quantum dots make them applied extensively in the field of optoelectronics applications. The PbTe is a very important and efficient thermoelectric material as well as considered for power creation applications through enhancing power factors via improvement in energy band engineering. The cubic NbTe with indirect band-gap semiconductor as well as ultra-high charge carrier mobility is prominent and excellent as compared to another 2-dimension semiconductor for ultra-fast optoelectronic application [8].

Theoretical materials have a wide range of applications such as efficient thermal properties. The parameters which determine the thermoelectric efficiency are dependent on different features such as Debye temperature (K), Enthalpy (U-U), Helmholtz free energy F(T), entropy (S-S), and heat capacity ( $C_p-C_v$ ) respectively. Telluride (Te) based compounds exhibit efficient properties which are unusual, as compared to other semiconducting materials [9-10]. The semiconducting CdTe, PbTe, and NbTe compounds show a narrow direct structure of bandgap at place G symmetry. Furthermore, depiction of the electronic, structural and optical properties of Telluride (Te) based compounds but there is a knowledge gap about their thermal characteristics. An accurate explanation of the thermal properties of cubic Telluride (Te) based compounds XTe (X= Pb, Cd, Nb) are crucial because they have a significant influence in defining the characteristics any materials. According to best our information, literature to yet has no theoretical studies on the electrical, optical, or thermal behaviour of these Telluride (Te) based XTe (X= Pb, Cd, or Nb) compounds. The main goal of the current work is to provide some substantial and relevant information to the data that has been presented about the electrical, structural, and thermal properties of compounds based on Telluride (Te) through simulation utilising CASTEP software and density functional theory. The purpose of this research is to investigate whether Telluride (Te) based compounds are efficient and appropriate for applications in optoelectronic devices. The findings show that the energy band gap of compounds based on Telluride (Te) is trending decrement. Telluride (Te) based compounds XTe (X= Pb, Cd, Nb) are more reliable and suitable materials for optoelectronic applications due to their promising optical conductivity, heat capacity, entropy, and enthalpy.

## 2. Computational approach:

The flawless cubic (Pm3m) rally of labeled Telluride (Te) based compounds XTe (X= Pb, Cd, Nb) was simulated through CASTEP software with PBE+GGA approximation. In the (X= Cd<sup>+</sup>, Pb<sup>+</sup> and Nb<sup>+</sup>) is positioned at coordinates (0.5, 0.5, 0.5) moreover Te<sup>+</sup> is located at coordinates of the crystal structure (0, 0.5, 0), furthermore at face-centered (0, 0.5, 0) as shown in Fig.1 (a-c). The ensuing lattice parameter is 3.7631 Å, which matches very well with the given value of 3.80. The electronic configuration of Pb, Cd, Nb, and Te respectively. To explore the effect of Cd, Pb and Nb of 1×1×1 super crystal tactic was used to reduce boundary limitations. Furthermore, Te was substituted at center position, depending on the super-cells shown in Fig.1. The USP is often used to quantify the interaction between electrons and ions, although PBE proposed a GGA approach to assessing the interactions among electron exchangers. The USP approach

was utilized with cutoff energy 517 eV to calculate the geometry simulation. The Brillouin zone was build over 666  $k$ -points through the Monkhorst–Pack Grid (MPG). The converging precision was adjusted at  $2 \times 10^{-5}$  eV/atom. The domain of remnant forces was restricted to 2 meV/Å.

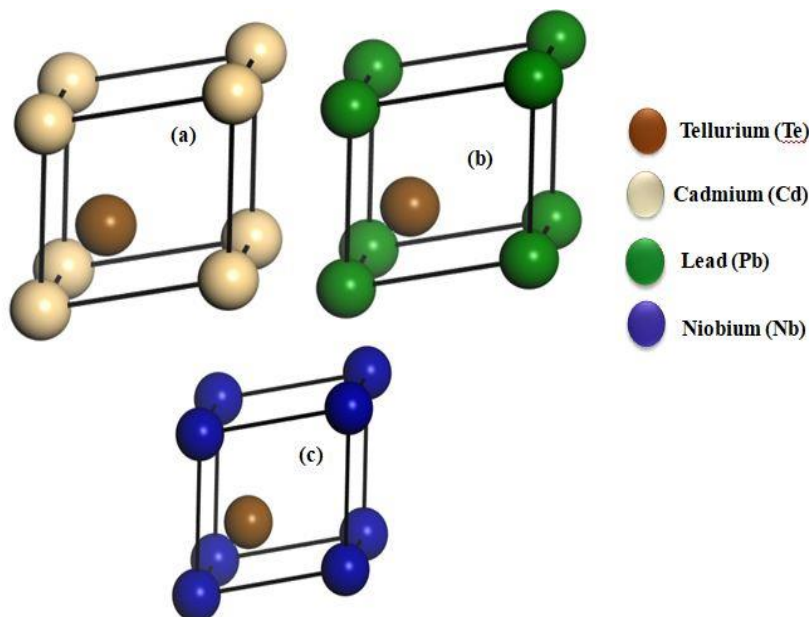


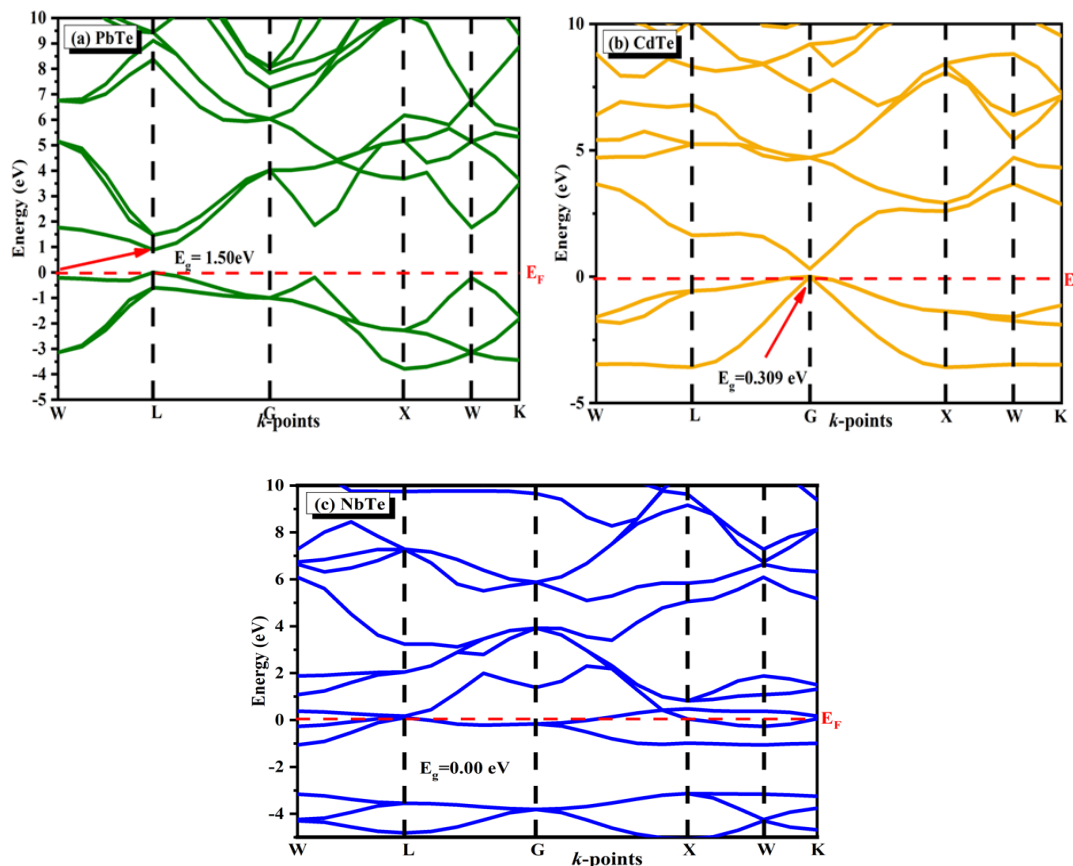
**Figure 1:** Supercell structure of (a) CdTe (b) PbTe and (c) NbTe.

### 3 Results and Discussion:

#### 3.1 Structure Analysis:

The simulated lattice structure parameters for pure CYF is gained which is  $a = b = c = 4.593 \text{ \AA}$ , through the Birch-Murnaghan equation. After geometry optimization, lattice constants are  $a = b = c = 4.60 \text{ \AA}$ , which have errors of about 0.15% related to the theoretical one, correspondingly as shown in Fig.1(a-c). The optimized position of the atoms is XTe ( $X = \text{Pb}^+, \text{Cd}^+$  and  $\text{Nb}^+$ ) are positioned at (0.5, 0.5, 0.5) and  $\text{Te}^+$  is placed at of the cell (0, 0.5, 0), while at face-centered (0, 0.5, 0), which have an error that cannot exceed more than 0.15%. These outcomes point out that our computational investigations are realistic, which certifies the reliability of our successive calculations. However, the designed lattice parameter of Telluride ( $\text{Te} = b = c = 4.47 \text{ \AA}$ ). After optimization, the lattice constants are  $a = b = c = 4.51 \text{ \AA}$  which have errors of about 0.88% related to the experimental ones, respectively.

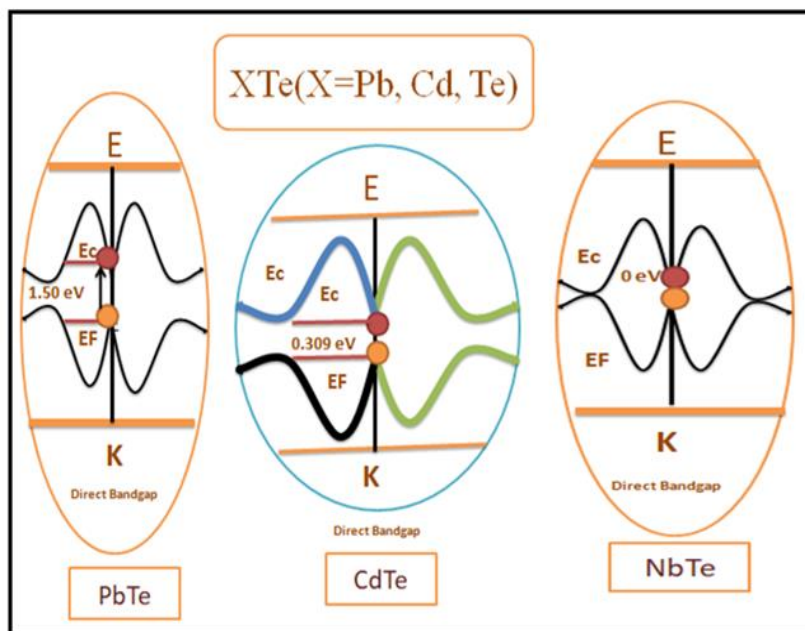
3.2 Electronic properties:



**Figure 2:** Band structures of Telluride (Te) based compounds (a) PbTe (b) CdTe and (c) NbTe

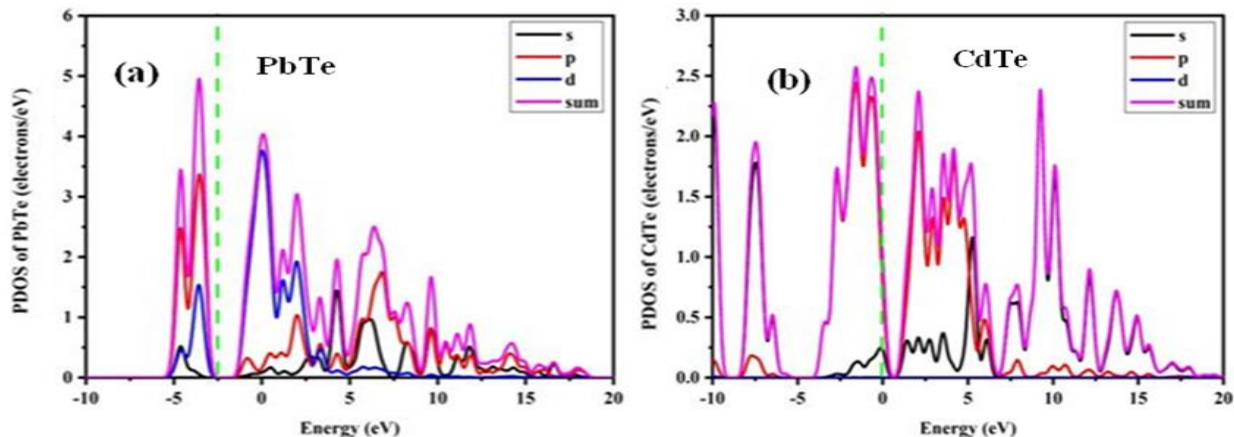
The energy eigenvalues of concerning electronic structure participate in figure out Fermi levels, which decide the material is conductor or semiconductor. The energy bands of Telluride (Te) based compounds XTe (X=Cd, Pb, Nb) are shown in Fig. 2 (a-c). The maxima (VBM) upper edge of valence band and minima (CBM) lower edge of conduction band site at different k points, this decide Telluride (Te) based compounds XTe (X= Pb, Cd, Nb) are narrow band-gap semiconductor compound. The whole profile shows that the characteristics of XTe (X= Pb, Cd, Nb) compounds are the similar by simulation. In the Telluride (Te) based compounds, VBM (crest) and CBM (trough) position on the same symmetry L and G symmetries of the Brillion zone in PbTe, CdTe respectively indicating the cubic materials have a direct band gap as presented in Fig. 2(a-c). The direct band gap for Telluride (Te) based compounds XTe (X=) are 1.50eV, 0.309 eV, and 0.00 eV respectively showing these compounds have narrow band-gap semiconductor behavior for optoelectronic device applications.

The band structure for Telluride (Te) based compounds XTe (X= Pb, Cd, Nb) are same in shape with the appropriate symmetry lines with minor variation in energy levels at G and L symmetry position. These results indicate that CBM is slightly shifting toward the ( $E_F$ ) Fermi energy level. The band gap for XTe (X= Pb, Cd, Nb) has been decreased by 1.50 eV, 0.309 eV, and 0.00 eV corresponding doping X= Pb, Cd, Nb, respectively as shown in Fig.3(a-c).



**Figure 3 (a-c):** Schematic diagram of direct bandgap structures of Telluride (Te) based compounds (a) PbTe, (b) CdTe and (c) NbTe.

The Bandgap decrement with X= Pb, Cd, Nb is shown in Figs. 2(a-c) and Fig 3(a-c). Moreover, The CBM slightly move toward  $E_F$  to closer the band gap, with X= Pb, Cd, Nb. The direct band gap promising effect on optical characteristics as presented in Fig.5. In comparison the energy ( $E_g$ ) band gap is significantly contracted by X= Pb, Cd, Nb are used. The VMB and CMB of X= Pb, Cd, Nb are located at L and G points in the 1<sup>st</sup> Brillion zone. The decrement in the  $E_g$  bandgap is because of appearance of newly energy states nearby the energy Fermi  $E_F$  level. Furthmore, all the facts are shown , in DOS and PDOS findings as shown in Fig. 4 (a-c). These results conclude that the  $E_g$  of Telluride (Te) based compounds XTe (X= Pb, Cd, Nb) are prominent, and outstanding for optoelectronic device applications.



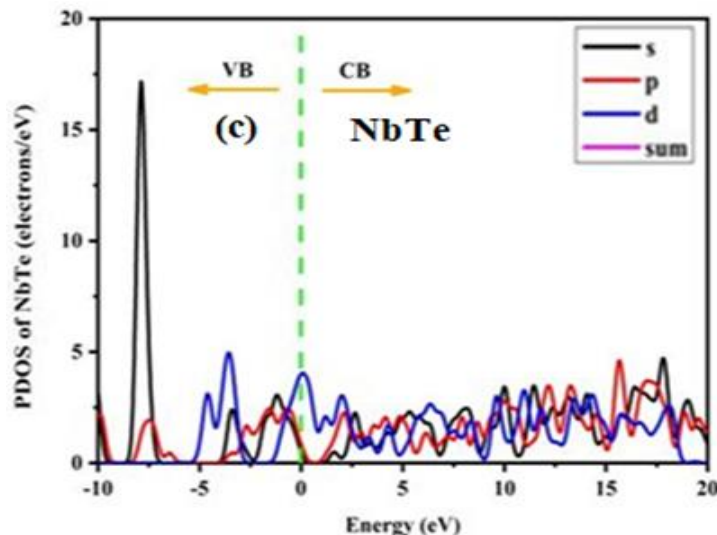


**Figure 4 (a-c):** Partial density of states (PDOS) of Telluride (Te) based compounds (a) PbTe, (b) CdTe, and (c) NbTe

Fig.4(a-c): shows that by substituting XTe (X= Pb, Cd, Nb) decrement in energy bandgap, this predicting that Telluride (Te) based compounds are proficient for optoelectronic device applications. The energy band gap scheme represents that per unit energy are calculated by total density of states moreover ions role of various band structures are examined through PDS. The decrement in the band gap can be explained using the TDOS and PDOS. Fig-4(a-d) represent that the elemental examination of XTe (X= Pb, Cd, Nb) PDOS. These graphs delegate that sum of states participate important role to the CB and have the steepest peaks represent at -5.25 eV and 15.343 eV, correspondingly. Furthermore, the Pb, Cd, and Nb-s states of Telluride (Te) based compounds have smaller peaks placed at -5.eV and 15 eV, correspondingly, and fascinatingly P-state in valance band is greater impact as compare to CB. Additionally, the sum of states has a proficient effect on conduction band, Therefore, the CB and VB are significantly exaggerated by the accretion of states in Telluride (Te) based compounds XTe (X= Pb, Cd, Nb). By the help of energy bandgap results we can indicate that PDOS slightly shift towards smaller energies as a result foremost to decrement trend in energy band gap, which is also simplified the optical explanation is given below.

### 3.3 Optical Properties:

Telluride (Te) based compounds XTe (X= Pb, Cd, Nb) have intriguing optical characteristics and are widely used in optoelectronic devices. The complex  $\varepsilon(\omega)$  dielectric calculations describes the behavior of Telluride (Te) based materials XTe (X= Pb, Cd, Nb) toward an electric field. It consists of two parts: the real and the imaginary of the dielectric terms, both of which depend on the optical band structure of the crystal.

The optical properties of Telluride (Te) based materials can be used to explain XTe (X= Pb, Cd, and Nb) compounds through the electronic structure, along with relative permittivity, refractive index, reflectivity, energy loss function and coefficient of absorption. These properties are very meaningful in signifying appropriateness of Telluride (Te) based compounds XTe (X= Pb, Cd, Nb) material in optoelectronic and electronic devices. All of the optical properties are result of the dealings of materials (Telluride material) and electromagnetic waves. All these optical results are connected to each other's; the complex term of dielectric is used which is given by [11-12].

$$\varepsilon(\omega) = (\varepsilon_1(\omega) + i\varepsilon_2(\omega)) \tag{1}$$

Equations (2) and (3) can be used to calculate the the dielectric function's RDF ( $\varepsilon_1(\omega)$ ) and IDF  $\varepsilon_2(\omega)$  in order to analyse the optical response [13-14].

$$\varepsilon_2(\omega) = -\frac{Ve^2}{2\pi\hbar m^2 \omega^2} \int d^3k \sum_{nm'} 1 \langle kn|P|k\tilde{n} \rangle I^2 f(k) \times (1 - f(k\tilde{n})) \delta(E_{kn} - E_{k\tilde{n}} - \hbar\omega) \tag{2}$$

$$(\varepsilon_1(\omega) = 1 + \frac{2}{\pi} P \int_0^\infty \frac{\omega' \varepsilon_2(\omega') d\omega'}{\omega'^2 - \omega^2} = n^2(\omega) - k^2(\omega), \tag{3}$$

$$a(\omega) = \frac{4k\pi}{\lambda} = \frac{\omega}{nc} \varepsilon_2(\omega), \tag{4}$$

$$a(\omega) = 2\omega k(\omega) = \sqrt{2} [\{\varepsilon_1(\omega)^2 + \varepsilon_2(\omega)^2\}^{1/2} - \varepsilon_1(\omega)]^{1/2} \tag{5}$$

$$L(\omega) = \frac{\varepsilon_2}{\varepsilon_1(\omega)^2 + \varepsilon_2(\omega)^2} \tag{6}$$

$$I(\omega) = \sqrt{2}\omega(\sqrt{\varepsilon_1(\omega)^2 + \varepsilon_2(\omega)^2} - \varepsilon_1(\omega))^{1/2} \tag{7}$$

$$n(\omega) = \left(\frac{1}{\sqrt{2}}\right) (\sqrt{\varepsilon_1(\omega)^2 + \varepsilon_2(\omega)^2} - \varepsilon_1(\omega))^{1/2} \tag{8}$$

$$K(\omega) = \frac{I(\omega)}{2\omega} \tag{9}$$

$$r(\omega) = \frac{n+iK-1}{n+iK+1} \tag{10}$$

$$\sqrt{\varepsilon(\omega)} = n(\omega) + iK(\omega) = N(\omega) \tag{11}$$

$$\varepsilon_1(\omega) = n^2 - K^2 \tag{12}$$

$$\varepsilon_2(\omega) = 2nK \tag{13}$$

The absorbance of Telluride (Te) based material is increasing with doped XTe (X= Pb, Cd, Nb) elements as presented in Fig.5(b). The photon energy increment by increasing doped XTe (X= Pb, Cd, Nb) elements, the absorption coefficient of Telluride (Te) based material rises of XTe (X= Pb, Cd, Nb) materials respectively. On the other side reflectivity of Telluride (Te) based material is decreasing as shown in Fig 5(d). The findings show that materials based on Telluride (Te) have proficient optical conductivity and absorbance, making them more reliable and suitable for optoelectronic applications.

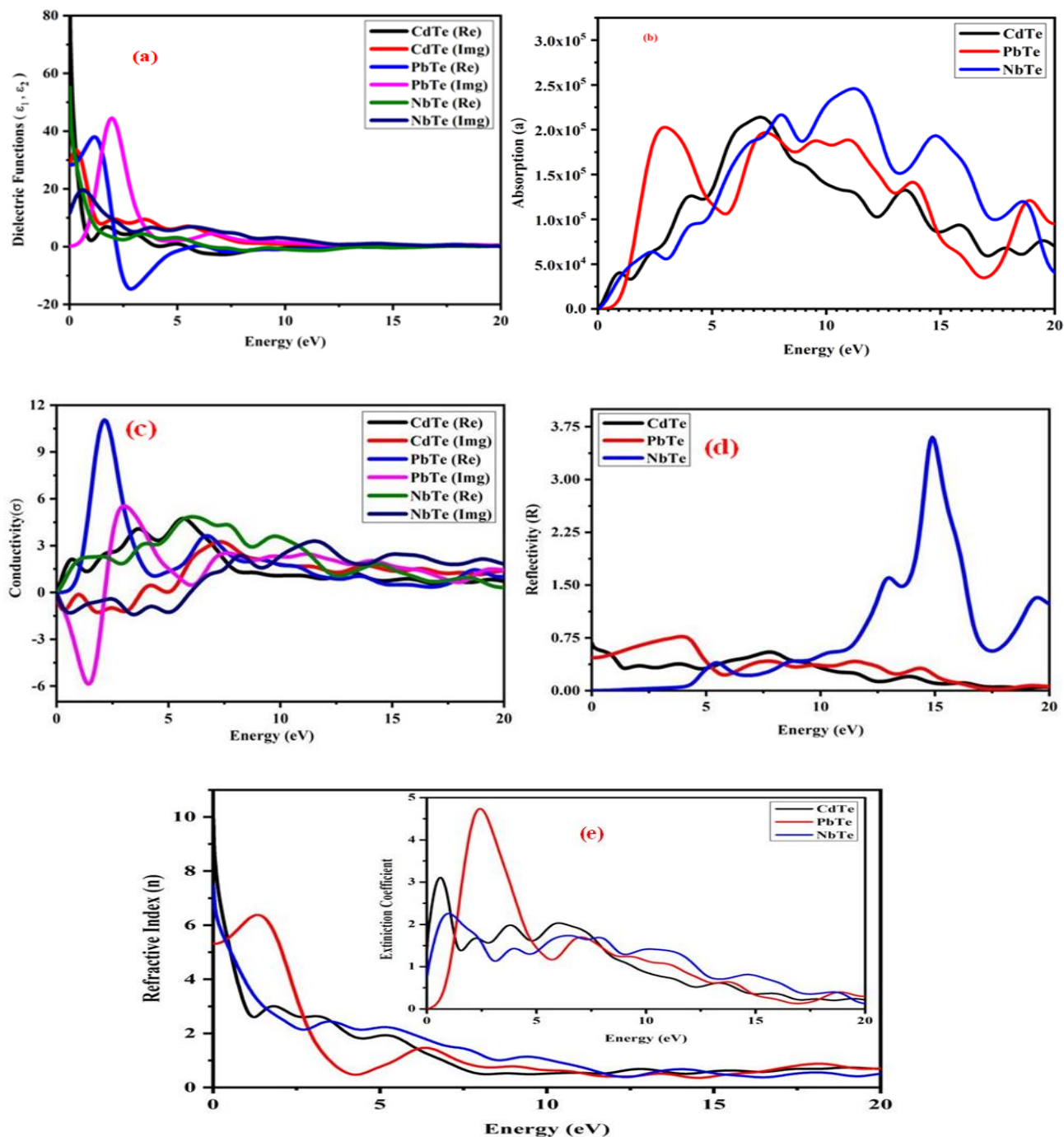


**Figure.5(a-e):** (a) Dielectric functions (b) absorption (c) conductivity (d) reflectivity and (e) refractive index of Telluride (Te) based compounds

Any material's reflectivity can be utilized to study the behavior of its surface. The reflectivity surface behavior of Telluride (Te) based material with doped XTe (X= Pb, Cd, Nb) is shown in Fig.5(d). The result present that reflectivity peaks slightly shift toward the larger values of frequency of XTe (X= Pb, Cd, Nb)

materials. As the frequency increases, the reflectance rapidly decreases from 3.5 to 0.75. The ability of any material to absorb luminescent electromagnetic waves in contrast to photons of the proper energy ( $E = \hbar\omega$ ), is closely related to the absorption of that material. In addition, when the material comes into range with incident photons, the energy dissipation is described by the energy loss function  $L(\omega)$ .

**3.3 Thermal Properties:**

To study the thermodynamic behavior of Telluride (Te) based material with doped XTe (X= Pb, Cd, Nb) through different thermodynamic functions such as heat capacity at constant volume  $C_v$ , heat capacity at constant Pressure  $C_p$ , enthalpy, vibration entropy  $S(T)$ , Internal energy  $U(T)$ , Helmholtz free energy  $F(T)$  as shown in Fig. 6(a-e). The heat capacity  $C_v$  at constant volume is given by [15-16].

$$C_v = \gamma K_B \int_0^\infty d\omega g(\omega) \left(\frac{\hbar\omega}{K_B T}\right)^2 \frac{\exp\left(\frac{\hbar\omega}{K_B T}\right)}{\left[\exp\left(\frac{\hbar\omega}{K_B T}\right) - 1\right]^2} \tag{14}$$

Here  $\gamma$  is representing the degree of freedom and  $g(\omega)$  is density of states of unit cell. Moreover,  $\hbar$  and  $K_B$  are representing Planks constant and Boltzmann constant respectively. The  $C_v$  limit at temperature  $0^\circ\text{K}$  furthermore maximum temperature are 0 and  $K_B T$  correspondingly. The relation between  $C_p$  and  $C_v$  at constant (Pressure and Volume) of quasi-harmonic approach is given by [17-18]

$$C_p - C_v = \alpha^2(T) BVT \tag{15}$$

In the above equation “ $\alpha$ ” is the thermal expansion coefficient of constant volume defined as  $(1/V)(\partial V/\partial T)$  moreover  $V$  is volume of system. The vibration entropy  $S(T)$  can be calculated at the finite temperature [19-23].

$$S(T) = \gamma K_B \int_0^\infty g(\omega) \left\{ \left(\frac{\hbar\omega}{2K_B T}\right) \left[ \coth\left(\frac{\hbar\omega}{K_B T}\right) - 1 \right] - \ln \left[ 1 - \exp\left(\frac{-\hbar\omega}{K_B T}\right) \right] \right\} d\omega \tag{16}$$

The internal energy  $U(T)$  of Telluride (Te) unit cell be measured through given equation.

$$U(T) = \frac{1}{2} r \int_0^\infty \hbar\omega g(\omega) \coth\left(\frac{\hbar\omega}{K_B T}\right) \tag{17}$$

All above calculated thermodynamic functions, we can measured Helmholtz free energy  $F(T)$  of Telluride (Te) unit cell.

$$F(T) = E_{elec} + U(T) - TS(T) \tag{18}$$

In above equation  $E_{elec}$  is representing the electronic energy of the Telluride (Te) unit cell can be calculated through first principles total-energy of Telluride (Te) based compounds XTe (X= Pb, Cd, Nb) calculations. In the current study the thermal expansion impact which is associated to the enharmonic trend of Telluride (Te) based compounds XTe (X= Pb, Cd, Nb). Furthermore, quasi-harmonic approximation (QHA), in which phonons of Telluride (Te) compounds are pretended as harmonic but dependent volume. The Telluride (Te) compounds unit cell are compressed and expended to set of fix volumes through positions of atoms and shape of the unit cell. The equilibrium volume of unit cell at appropriate temperature  $T$  is attained through minimizing the free energy of the unit cell. The calculated free energy versus temperature of Telluride (Te) based compounds XTe (X= Pb, Cd, Nb) as shown in Fig.5(c). PbTe has proficient thermal stability at high temperature. It is astounded that PbTe show prominent thermal stability at high temperature such as at above 150 K. Quasi-harmonic approximation (QHA) is only applicable when the temperature is much smaller than melting point where enharmonic impact is foremost.

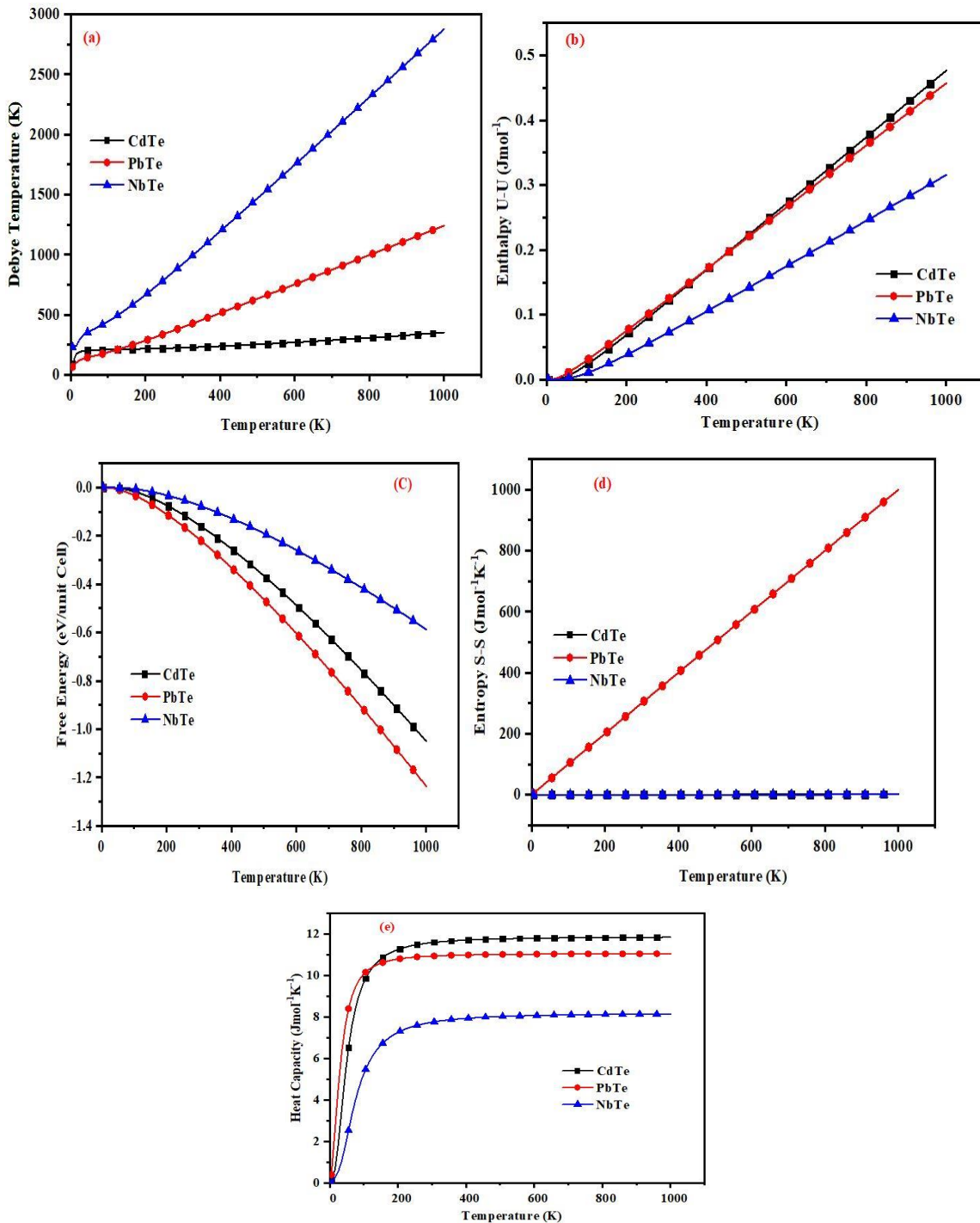


**Figure.6(a-e):** (a) Debye temperature (b) enthalpy (c) free energy (d) entropy (e) heat capacity of Telluride (Te) based compounds XTe (X= Pb, Cd, Nb).

100K temperature. According to the findings, materials based on Telluride (Te) have excellent heat capacity and are more reliable and suitable for optoelectronic applications.

#### 4 CONCLUSION:

Under the First-principles exploration Pb, Cd, and Nb are appropriate periodic elements for bandgap decrement in XTe materials. The bandgap of XTe (X= Pb, Cd, Nb) was originate significantly decrement from 1.50 eV to 0.00 eV. Niobium (Nb) is more advantageous than Pb and Cd. By substituting of X= Pb, Cd, Nb at the corner sites in XTe (X= Pb, Cd, Nb) additional gamma sites were participated in the electronic energy band gap ( $E_g$ ). It is also examined that optical peaks shifted toward larger energy due to decrement in the band gap. Thermal impact on macroscopic properties of XTe (X= Pb, Cd, Nb) compounds are predicted using the quasi-harmonic Debye model these materials are thermally stable. The variations of the enthalpy (U-U), entropy (S-S), heat capacity, Debye temperature, and free energy with temperature function are obtained successfully. Moreover, small band-gap semiconducting Telluride (Te) based materials reveal low thermal conductivities at a prominent temperature which is curious for simple cubic structured materials. In the future inspective scope, these Telluride based materials find great potential because of very less energy production possessions, moreover present computed work is awaiting lab work.

#### Ethics Approval

The Research is not involving studies on human or their data.

#### Availability of data:

The data that support the findings of this study are available from the corresponding author upon reasonable request.

#### Conflict of interest

No conflict of interest

#### Competing interests:

The authors declare that they have no known competing financial interests or personal relationships that could have appeared to influence the work reported in this paper.

#### References:

- [1] M. C. Shaughnessy, N. C. Bartelt, J. A. Zimmerman, and J. D. Sugar, "Energetics and diffusion of gold in bismuth telluride-based thermoelectric compounds," *J. Appl. Phys.*, vol. 115, no. 6, 2014, doi: 10.1063/1.4865735.
- [2] M. H. Jameel et al., "A Comparative DFT Study of Bandgap Engineering and Tuning of Structural, Electronic, and Optical Properties of 2D WS<sub>2</sub>, PtS<sub>2</sub>, and MoS<sub>2</sub> between WSe<sub>2</sub>, PtSe<sub>2</sub>, and MoSe<sub>2</sub> Materials for Photocatalytic and Solar Cell Applications," *J. Inorg. Organomet. Polym. Mater.*, no. August, 2023, doi: 10.1007/s10904-023-02828-0.
- [3] Turki Jalil, A., Emad Al Qurabiy, H., Hussain Dilfy, S., Oudah Meza, S., Aravindhan, S., M Kadhim, M., & M Aljeboree, A. (2021). CuO/ZrO<sub>2</sub> nanocomposites: facile synthesis, characterization and photocatalytic degradation of tetracycline antibiotic. *Journal of Nanostructures*, 11(2), 333-346
- [4] Hasan Jabbar, A., Oudah Mezan, S., Alameri, A. A., Prakaash, A. S., Mohammed Baqir Al-Dhalimy, A., & Younes, A. (2023). Fe<sub>3</sub>O<sub>4</sub>@ Diamine-CuI Nanocomposite: A Novel and Highly Reusable Nanomagnetic Catalyst for Ecofriendly Synthesis of Triaryl Imidazoles. *Polycyclic Aromatic Compounds*, 1-17.

- [5] Mezan, S. O., Jabbar, A. H., Jabbare, A. T., Abs, S. M. A., Roslan, M. S., & Agam, M. A. (2022, October). Synthesis and enhancement of morphological and structural properties of zinc sulphide thin films nanoparticle for solar cell application. In AIP Conference Proceedings (Vol. 2398, No. 1). AIP Publishing.
- [6] M. H. Jameel et al., "Investigation of structural, electronic and optical properties of two-dimensional MoS<sub>2</sub>-doped-V<sub>2</sub>O<sub>5</sub> composites for photocatalytic application: a density functional theory study," Royal Society open science, 10(7),2023, 230503. <https://doi.org/10.1098/rsos.230503>.
- [7] R. E. Taylor et al., "A combined NMR and DFT study of narrow gap semiconductors: The case of PbTe," J. Phys. Chem. C, vol. 117, no. 17, pp. 8959–8967, 2013, doi: 10.1021/jp3101877.
- [8] Y. Gelbstein, Z. Dashevsky, and M. P. Dariel, "High performance n-type PbTe-based materials for thermoelectric applications," Phys. B Condens. Matter, vol. 363, no. 1–4, pp. 196–205, 2005, doi: 10.1016/j.physb.2005.03.022.
- [9] M. Serhan et al., Total iron measurement in human serum with a smartphone, vol. 2019-Novem. 2019.
- [10] M. H. Jameel et al., "A comparative DFT study of electronic and optical properties of Pb/Cd-doped LaVO<sub>4</sub> and Pb/Cd-LuVO<sub>4</sub> for electronic device applications," Comput. Condens. Matter, vol. 34, no. November 2022, p. e00773, 2023, doi: 10.1016/j.cocom.2022.e00773.
- [11] S. El Oualid et al., "Innovative design of bismuth-telluride-based thermoelectric micro-generators with high output power," Energy Environ. Sci., vol. 13, no. 10, pp. 3579–3591, 2020, doi: 10.1039/d0ee02579h.
- [12] B. K. Al-Rawi, S. M. Hameed, and M. A. M. Alsaadi, "Simulation of electronic structure and some properties of CdTe crystals using DFT," Mater. Sci. Forum, vol. 1021, no. April 2021, pp. 1–10, 2021, doi: 10.4028/www.scientific.net/MSF.1021.1.
- [13] M. H. Jameel, A. Rehman, M. S. bin Roslan, and M. A. Bin Agam, "To investigate the structural, electronic, optical and magnetic properties of Sr-doped KNbO<sub>3</sub> for perovskite solar cell applications: A DFT study," Phys. Scr., vol. 98, no. 5, 2023, doi: 10.1088/1402-4896/acc6fb.
- [14] J. P. Heremans et al., "Enhancement of thermoelectric efficiency in PbTe by distortion of the electronic density of states," Science (80-. ), vol. 321, no. 5888, pp. 554–557, 2008, doi: 10.1126/science.1159725.
- [15] F. M. Mohammed, F. I. Rashid, and shahad A. Shaaban, "Electronic Configuration and Charge Transfer Study in (CdTe)," Int. J. Electron. Commun. Eng., vol. 5, no. 5, pp. 1–5, 2018, doi: 10.14445/23488549/ijece-v5i5p101.
- [16] M. Hasnain, J. Muhammad, R. Mohd, and A. Bin, "Effect of external static pressure on structural , electronic , and optical properties of 2 - D hetero - junction - MoS<sub>2</sub> for a photocatalytic applications : A DFT study," Opt. Quantum Electron., vol. 2, pp. 1–14, 2023, doi: 10.1007/s11082-023-04853-2.
- [17] O. Cojocaru-Mirédin et al., "Role of Nanostructuring and Microstructuring in Silver Antimony Telluride Compounds for Thermoelectric Applications," ACS Appl. Mater. Interfaces, vol. 9, no. 17, pp. 14779–14790, 2017, doi: 10.1021/acsami.7b00689.
- [18] M. H. Jameel et al., "First principal calculations of electronic, optical and magnetic properties of cubic K<sub>1-x</sub>Y<sub>x</sub>NbO<sub>3</sub>(Y = Fe, Ni)," Phys. Scr., vol. 96, no. 12, 2021, doi: 10.1088/1402-4896/ac198d.

- [19] D. I. Bilc, S. D. Mahanti, and M. G. Kanatzidis, "Electronic transport properties of PbTe and AgPbm SbTe  $2+m$  systems," *Phys. Rev. B - Condens. Matter Mater. Phys.*, vol. 74, no. 12, 2006, doi: 10.1103/PhysRevB.74.125202.
- [20] A. H. Romero, E. K. U. Gross, M. J. Verstraete, and O. Hellman, "Thermal conductivity in PbTe from first principles," *Phys. Rev. B - Condens. Matter Mater. Phys.*, vol. 91, no. 21, 2015, doi: 10.1103/PhysRevB.91.214310.
- [21] Altajer, A. H., Efendi, S., Jabbar, A. H., Oudah Mezan, S., Thangavelu, L., M Kadhim, M., & F Alkai, A. M. (2021). Novel carbon quantum dots: Green and facile synthesis, characterization and its application in on-off-on fluorescent probes for ascorbic acid. *Journal of Nanostructures*, 11(2), 236-242.
- [22] G. J. Snyder, T. Caillat, and J. P. Fleurial, "Thermoelectric properties of the incommensurate layered semiconductor  $GexNbTe_2$ ," *J. Mater. Res.*, vol. 15, no. 12, pp. 2789–2793, 2000, doi: 10.1557/JMR.2000.0398.
- [23] Saleh, R. O., Mansouri, S., Hammoud, A., Rodrigues, P., Mezan, S. O., Deorari, M., & Shakir, M. N. (2023). Dual-mode colorimetric and fluorescence biosensors for the detection of foodborne bacteria. *Clinica Chimica Acta*, 117741..